# Optical characterization of high performance mirrors based on cavity ringdown time measurements with 6 degrees of freedom mirror positioning

N Gutierrez, J Degallaix, D Hofman, C Michel, L Pinard, J Morville, R Battesti, G Cagnoli

# Optical characterization of high performance mirrors based on cavity ringdown time measurements with 6 degrees of freedom mirror positioning

N.Gutierrez,[1, a)] J.Degallaix,[1] D.Hofman,[1] C.Michel,[1] L.Pinard,[1] J.Morville,[2] R.Battesti,[3] and G.Cagnoli[2]

[1)] *Université Lyon, Université Claude Bernard Lyon 1, CNRS, Laboratoire des Matériaux Avancés (LMA), IP2I Lyon / IN2P3, F-69622 Villeurbanne, France*

[2)] *Institut Lumière Matière, CNRS UMR5306, Université de Lyon, Université Lyon 1, F-69622 Villeurbanne, France*

[3)] *Laboratoire National des Champs Magnétiques Intenses (UPR 3228, CNRS-UPS-UGA-INSA), F-31400 Toulouse, France*

(Dated: 9 October 2023)

An instrument capable of measuring optical losses, transmission and radius of curvature of high reflectivity mirrors is presented. The measurement setup consists of two remote controlled hexapod systems with 6 degrees of freedom placed inside a vacuum enclosure. Mirror loss measurements are performed via cavity ring-down time method using a linear resonant two-mirror Fabry-Perot cavity configuration. The use of high-precision positioning systems enables cavity loss mapping by transversely scanning the position of the cavity end mirror. Mirror surfaces of up to 30 mm in diameter can be scanned and the cavity length can be tuned by 120 mm.

[a)] n.gutierrez@lma.in2p3.fr

## I. INTRODUCTION

High reflectivity, ultra-low-loss mirrors are critical components in reference cavities for ultra-stable lasers[1], probing opto-mechanical coupling[2] and gravitational wave detectors[3]. Advancements in coating and mirror polishing techniques have allowed the reduction of mirror optical losses to the order of 10 ppm (parts-per-million)[4]. However, punctual defects on a mirror's substrate or coating can introduce well localized losses and excess scattering detrimental to high accuracy laser optical applications.

While dedicated setups can characterise individually scattering or absorption losses, it is preferable to measure the total optical losses of the mirrors in real conditions, that means usually within a resonant cavity. Optical loss measurements based on cavity ringdown (CRD) is well suited to tackle this issue. While the nature of the defect detected cannot be known through CRD time measurements, total cavity losses can accurately be measured[5]. In the case of a two-mirror cavity, a third mirror can be used to permute and characterize all three possible optical cavities so that the losses of each individual mirror can be determined. Mirror losses measured in this manner will realistically translate to mirror performance under operating conditions. This technique is insensitive to laser power fluctuations and best suited for the characterization of high reflectivity mirrors as the detection of longer ringdown times is facilitated and does not require the use of fast photodetectors. In the case of very low loss mirrors, the instrument requires a vacuum chamber to remove the contribution of propagation losses in air which is of about 1 ppm per roundtrip for a 1.8m cavity and phase noise due to air turbulences. By mounting the end mirror of the Fabry-Perot cavity on high-precision positioning stages, reflectivity mappings of mirrors have been demonstrated in non-linear Fabry-Perot configurations such as V-shaped and four-mirror cavities[6,7]. Mirror loss mappings were later demonstrated using a linear two-mirror cavity with mirrors mounted on positioning systems with four degrees of movement freedom[8]. These types of systems have demonstrated to be precise enough to measure reflectivity and losses in HR components and for the detection of non-uniformities with sub-ppm accuracy[7]. While it is not possible to directly characterise large mirrors, these instruments can prove useful to validate the optical losses on small samples coated during the same run as the large mirrors (witness samples) or to validate improvements in optical performance resulting from new coating recipes during the research and development phase. In this paper we present

a new measurement bench for the complete characterization of mirror coatings. The setup consists of a linear Fabry-Perot cavity where each mirror is placed on a compact high-precision positioning stage with 6 degrees of freedom. The mirror surface can be scanned in order to measure mirror loss uniformity over surfaces of up to 30 mm in diameter. The positioning capabilities of the stages allow for measurements of mirror radius of curvature also demonstrated in this paper. Cavity length can be tuned by up to 120 mm to avoid higher order transverse modes which can skew mirror loss measurements. Lastly, mirror transmission can be measured thanks to the high dynamic range of our photodetectors at the output of the cavity.

## II. PRINCIPLE OF MEASUREMENT

Cavity ring-down time measurements are used as a mean of accurately measuring total cavity losses. In a cleanroom environment, a linear Fabry-Perot cavity configuration is implemented where the two mirrors that form the cavity are mounted on hexapods with 6 degrees of freedom of movement.

Cavity pre-alignment is performed manually. This process starts by mounting only the end cavity mirror and controlling its tilt angles to ensure that the laser beam reflected by the mirror is coincident with the incident beam (i.e. normal incidence of the laser on the mirror surface). The cavity input mirror is then placed on the input positioning system and the same procedure is applied. Fine tuning of the cavity alignment is performed while linearly scanning the laser frequency. The signal at the output of the cavity is photo-detected and visualized in real time while tilting the cavity mirrors to maximize the amplitude of the fundamental mode in the resonator while minimizing the presence of odd higher order modes. The cavity mode matching is achieved with a 2 lenses telescope. Good alignment and mode matching is considered when the amplitude of the first higher optical mode is less than 2% of the amplitude of the fundamental mode.

Ring-down time measurements are performed by first locking the laser frequency to a cavity resonance to maximize circulating intra-cavity power and then performing an instant shutoff of the incident laser light while recording the signal transmitted through the resonator. The intra-cavity photon decay time $\tau$ is related to the cavity's total losses $L_{tot}$ by the relation

$$\tau = \frac{1}{L_{tot} FSR} \tag{1}$$

which includes mirror transmission (extrinsic resonator losses) as well as mirror losses (intrinsic resonator losses). Propagation losses are not accounted for as they are negligible over a distance of 1.8 m in primary vacuum. $FSR$ is the cavity free spectral range defined as the frequency spacing between two adjacent resonances at a given wavelength and, for a two mirror cavity, is given by :

$$FSR = \frac{c}{2L} \tag{2}$$

With $c$ the speed of light in vacuum and $L$ the physical length of the cavity. The decay signal at the output of the cavity is recorded and fitted with a single exponential decay function using a least square fit method to determine photon lifetime inside the cavity. Mirror loss uniformity measurements are performed by raster scanning the end mirror of the cavity and measuring cavity ring-down time as a function of end mirror position. The positioning capabilities of the hexapods allow us to characterise mirror loss uniformity over surfaces of up to 30 mm in diameter.

Loss uniformity measurements over mirrors with spherical substrates require that the tilt angle of the mirror is adjusted after each translation to compensate for its radius of curvature $R$. Supposing that $R$ is much larger than a translation $d$, a tilt angle of $\theta = d/R$ is necessary to preserve cavity alignment with respect to the input beam after mirror translation. As will be shown later, the apparatus presented in this paper allows for radius of curvature measurements of spherical mirrors.

## III. EXPERIMENTAL SETUP

### A. Optical layout and control scheme

A detailed schematic of the experimental setup is depicted in figure 1. The path of light in the instrument is indicated by the red lines in figure 1 while the black lines indicate electrical connections between different blocks of the experimental setup. The laser used is a monochromatic continuous wave Nd:YAG solid-state Mephisto model from Coherent

operating at 1064 nm with a spectral line-width of 1 kHz over 100 ms before active frequency stabilization.

The active frequency stabilization method known as the Pound-Drever-Hall technique is implemented in order to lock the laser frequency to a cavity resonance[9,10]. This technique uses the laser light reflected by the resonator to generate a signed error signal that is proportional to the laser frequency detuning with respect to the closest cavity resonance. This error signal is fed to a cascade of controllers that act on the laser frequency via different mechanisms effectively locking it to a cavity resonance.

An acousto-optic modulator (AOM) set up in a double-pass configuration is employed to control the frequency and amplitude of the laser light at the input of the cavity[11,12]. The radio frequency (RF) signal fed to the AOM is generated and controlled through a voltage-controlled oscillator (VCO). The frequency of this RF signal controls the frequency shift of the laser with respect to the cavity resonance while the amplitude of the RF signal modulates the power of the optical signal at the input of the cavity. At the output of the AOM system a polarization maintaining optical fiber used in transmission serves two purposes. First, it acts as a mode cleaner, ensuring that only the fundamental spatial mode of the laser light enters the EOM used to generate the PDH error signal. Second, it converts any positional and beam pointing fluctuations of light coming from the double-pass AOM into optical power fluctuations that can easily be corrected with an active feedback loop acting on the RF power of the AOM drive signal. With the use of a double-pass AOM, the laser power directed into the Fabry-Perot cavity can be extinguished in less than 2 µs which is already 2 orders of magnitude smaller than the ring-down times measured. This fast shutoff time is achieved by applying a 0 V drive signal to the AOM which immediately deviates the laser beam at the input of the mode cleaning fiber from its path.

At the output of the fiber, a polarizer is placed to ensure that the polarization of light is purely linear and aligned with a neutral axis of the Electro-Optic Modulator in order to minimise residual amplitude modulation.

PDH error signal generation as well as Laser frequency stabilization are performed using a set of integrated modules from SISYPH[13] consisting of an RF frequency mixer and a DC-error controller for error signal generation and an auto-lock controller, a piezo compensator and a high-speed compensator for laser frequency control. The frequency control of the laser beam entering the cavity is performed using multiple actuators depending on the frequency

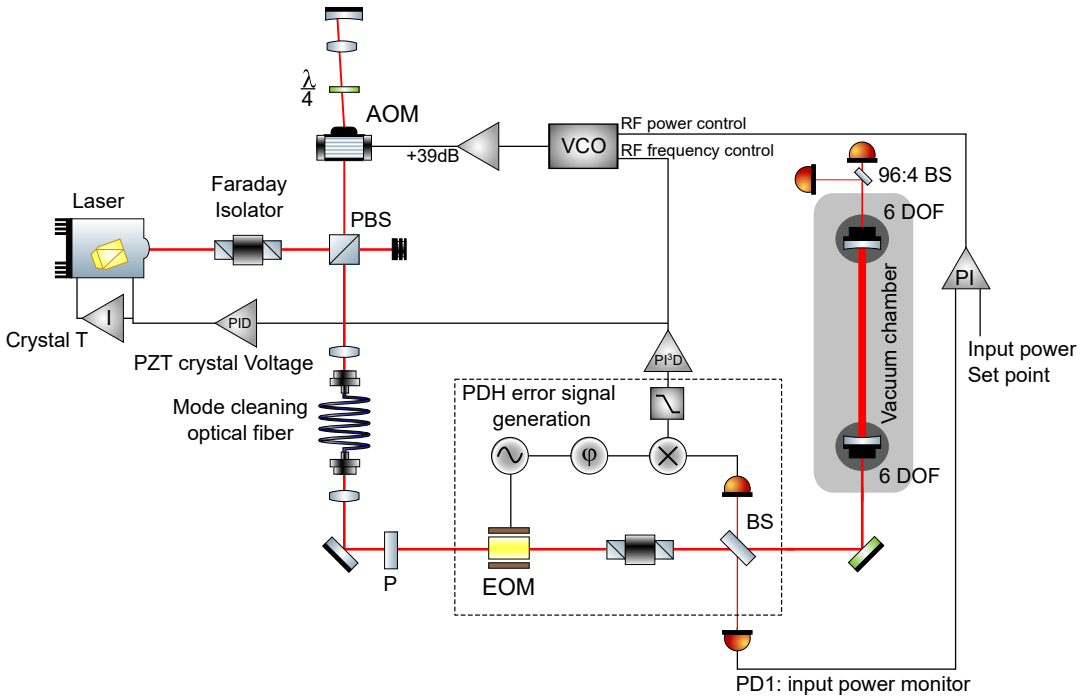


FIG. 1. Schematic of the mirror characterization instrument. AOM: Acousto-optic modulator; PBS: Polarization beam splitter; P: Polarizer; EOM: Electro-optic modulator; PDH: Pound-Drever-Hall; BS: Beamsplitter; PD: Photodetector; 6DOF: 6 Degrees of freedom positioning system; VCO: Voltage Controlled Oscillator.

and dynamic range of the targeted control. The high-speed actuator consists of a PI$^3$D controller that acts on the frequency of the RF signal fed to the double-pass AOM system allowing for fast corrections of the laser frequency albeit with a low dynamic range. The low frequency error signal is fed to a PID controller that acts directly on the voltage applied to the piezo crystal of the laser to control its frequency over a larger range. This low frequency path is used to desaturate the high-speed loop that controls the frequency of the signal fed to the double-pass AOM system. Lastly, the error signal is fed to an integral (I) controller that acts on the temperature of the laser crystal to correct low frequency fluctuations of the laser frequency ensuring long-term operation.

The auto-lock controller serves as an electronically controlled switch that turns on or off the the action of the PDH. In our experiment, this controller is configured so that it turns on the frequency control loop of the PDH as soon as the high gain photodiode at the output of the cavity detects an amount of optical power greater than a user-set threshold. This optical power threshold is set as greater than the optical power transmitted through

the cavity when the laser resonates with higher order cavity modes. This ensures that the PDH system will only attempt to lock the laser frequency to the cavity fundamental modes effectively ignoring the cavity higher order modes that may remain from imperfect alignment or mode-mismatching.

The signal transmitted through the cavity is separated by a 96:4 beamsplitter and focused into two photodetectors. The 4% tap power is directed into a high-speed and high gain photodetector model OE200 from Femto with gain set up to saturate whenever the frequency approaches resonance with the cavity and acts as a trigger to turn on the frequency correction loop described above. The remaining power transmitted through the cavity is directed into a low noise photodetector Model 2053 from New Focus that is used to measure the power transmitted through the cavity. The response time of both photo detectors was measured a priori and determined to be of the order of 1µs which is vastly fast enough for cavity ring-down time measurements of the order of hundreds of microseconds. Both signals are recorded using a National Instruments PCIe-6361 data acquisition card with 16 bit analog-to-digital converter resolution and using a 500 kHz sample frequency. Data treatment is performed automatically with a MATLAB program. The Fabry-Perot cavity is 1.80 m in length measured using the technique described in annex B and contained inside a vacuum tank as shown in figure 2. Operation of the cavity under vacuum conditions reduces acoustic noise, suppresses optical propagation losses between the two mirrors and helps avoid contamination of the mirror surfaces. Operation under vacuum conditions is crucial for our application as even the small propagation losses in air or any kind of accidental contamination of the mirror's surface can have a non-negligible impact on the measured ringdown time. Before performing ring-down time measurements, a primary vacuum pump is used to achieve a pressure of under 1 mbar inside the vacuum tank. The pump is then turned off and kept turned off for the duration of the measurements to avoid the transmission of mechanical vibrations from the pump to the vacuum tank. In addition to this, the vacuum tank containing the cavity is fixed on top of an optical table with high load capacity pneumatic isolation legs to mitigate any potential mechanical perturbations during operation. The experiment is carried in a clean room environment up to ISO-5 standard to maintain the purity of the tested optics especially during the process of installing and removing cavity mirrors.

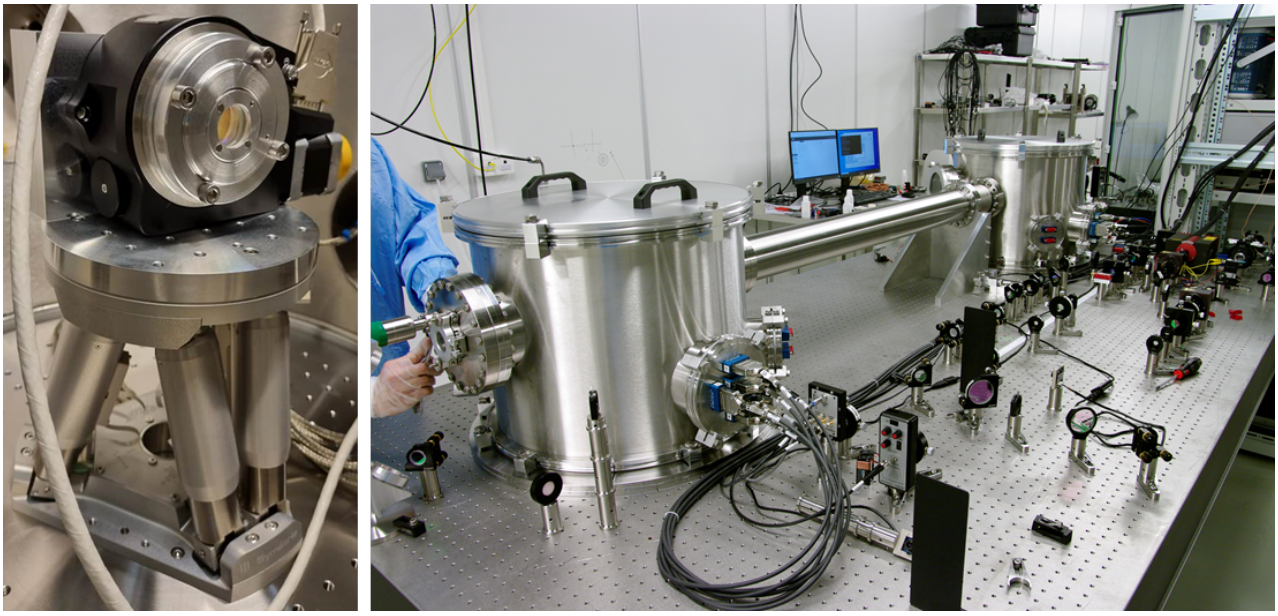

FIG. 2. Left: Photograph of the mirror positioning system. A custom made mirror mount is bolted on high precision rotation stage intended for future upgrades of the measurement instrument. Right: Photograph of the test bench. The cylindrical vacuum tanks contain the mirror positioning systems.

### B. Positioning system

The novelty of the measurement instrument presented in this paper lies in the positioning capabilities of the systems that make up the Fabry-Perot cavity. As is shown in figure 2. left, each mirror positioning system consists of a vacuum compatible hexapod model BORA from SYMMETRY with 0.1 µm positional accuracy and 2 µrad rotation accuracy and a low wobble rotation stage model L611-V6 from Physik Instrumente intended for future upgrades of the measurement instrument. The hexapods are custom-built to our specifications to have a larger travel range than the standard model. The hexapods are capable of performing ±30 mm translations on the plane of the moving platform (X and Y directions) and ±15 mm normal to the moving platform (Z direction). Each positioning system is controlled remotely via MATLAB.

The hexapods having 6 degrees of movement freedom allow for the scanning of the Fabry-Perot cavity length for distances of up to 120 mm and areas tranverse to the axis of the cavity of up to 30 mm in diameter. Simulations with a FFT propagation package have shown the

importance of having precise control over cavity length especially when large mirrors are used as high order mode degeneracy can drastically increase cavity losses for specific geometric configurations, thus skewing mirror loss measurements via ring-down time[14].

For each hexapod, a center of rotation and a coordinate system have to be defined with respect to its mobile platform. It is very important to define the center of rotation of the hexapod as the center of the coated surface of the mirror mounted on the positioning system. The mechanical drawings of the custom mirror mounts were used to define the position of the center of rotation. The dimensions of the mirror mounts were carefully measured to corroborate that their measurements correctly match their correspondent mechanical drawings.

## IV. RESULTS AND DISCUSSION

The measurement instrument was used to characterize two mirrors deposited on sapphire substrates with a radius of curvature of 8 m as specified by the polisher. The substrates, acquired from COASTLINE optics[15], have a roughness under 0.1 nm RMS and a flatness of $\lambda/20$. Mirror coating was performed at LMA (Laboratory of Advanced Materials) by Ion Beam Sputtering (IBS) to deposit a Bragg mirror using layers of silica as low index material and tantalum doped titanium dioxide as high index material. Layer thickness was controlled to center the reflection spectrum of the mirrors at 1064 nm in order to match our laser frequency. Both cavity mirrors were coated during the same run in the largest coating machine at LMA to guarantee an outstanding coating uniformity[16].

Radius of curvature as a well as mirror transmission measurements can be performed by only mounting the end cavity mirror. After mounting and alignment of the two cavity mirrors, total cavity losses are measured as cavity length is scanned to make sure that the geometry of the cavity does not support degenerate transverse modes that could negatively impact mirror loss measurements. Finally, cavity losses are measured as end mirror position is raster scanned transverse to the cavity axis in order to characterise mirror loss uniformity.

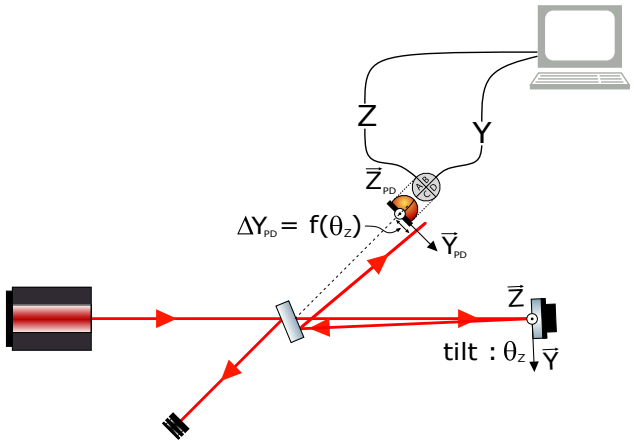


FIG. 3. Schematic of radius of curvature and transmission measurement setup.

### A. Radius of curvature measurements

When characterizing spherical mirrors, pure translations of the mirrors normal to the cavity axis produce a misalignment of the cavity due to the mirror's radius of curvature. This effect is circumvented by tilting the cavity mirror after each translation to restore the optimal alignment.

The mirror's radius of curvature is measured using the experimental setup represented in figure 3. Only the end mirror is installed and the beam reflected is aligned to fall at the center of a four-quadrant photodetector. The mirror is then translated by a distance $d$ along a given direction (Y or Z) and tilted around the axis orthogonal to the translation vector (by $\theta_z$ or $\theta_y$ respectively) while recording the reflected beam position on the four quadrant photo-detector. The zero-crossings on the four quadrant photo-detector (4Q-PD) signal indicate the value of $\theta = \theta_0$ for which the laser beam impacts the mirror at normal incidence. The radius of curvature of the mirror is then given by $R = d/\theta_0$.

Figure 4 shows the 4Q-PD vertical signal $V_z$ for three different mirror positions as the measured mirror is continuously tilted around the $y$ (horizontal) axis of the hexapod. The red lines correspond to a linear interpolation around the zero-crossings of the 4Q-PD signal used to find an accurate value of $\theta_0$ for which the 4Q-PD signal crosses zero (i.e. the mirror angle $\theta_y$ that produces a normal incidence of the laser on the mirror). In figure 5, $\theta_0$ is plotted for five different mirror transverse positions. The data is then fitted with a linear function in order to extract the value of the radius of curvature $R$ which is given by the

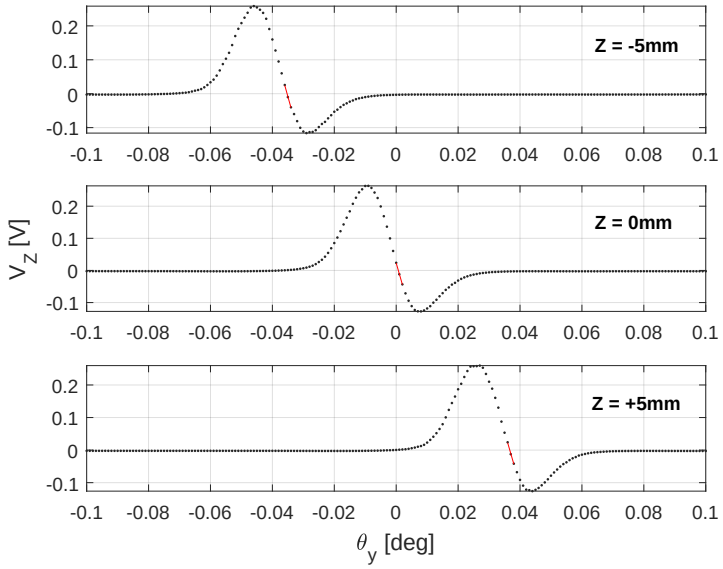


FIG. 4. Four quadrant photo-detector signal recorded as the mirror is tilted around the $y$ axis of the hexapod (tilt of $\theta_y$) for three different mirror positions $\Delta_z = -5\,\text{mm}$; $\Delta_z = 0\,\text{mm}$ $\Delta_z = +5\,\text{mm}$.

inverse of the slope of the linear fit and found to be 7.95 m on the cavity output mirror, to be compared to the 8 m specified to the polisher. This small difference is well within the polishing tolerances expected to be less than 0.2 m.

### B. Transmission measurements

Mirror transmission is measured using the same configuration as in the previous section. A variable gain photodetector with a conversion gain spanning from $1 \times 10^3\,\text{V/W}$ to $1 \times 10^{11}\,\text{V/W}$ is added to measure the optical power transmitted through the mirror. After the transmitted optical power is measured, the mirror is removed and incident optical power is measured using a lower gain setting on the photodetector. The mirror transmission is given by the ratio of transmitted to incident optical power which is measured to be of 8.5 ppm for both mirrors using this technique. For verification, mirror transmission measurements were performed alternatively using a complete angle scatter instrument (CASI) which yielded transmission measurement results of 8.2 ppm and 8.15 ppm for end and input mirrors respectively. While the CASI instrument yields more accurate transmission results, it is possible to infer that the transmission measurement method presented in this section

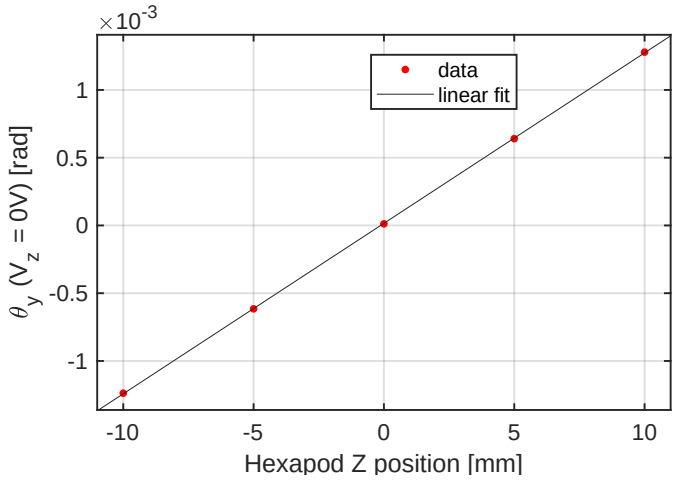


FIG. 5. Mirror tilt angle $\theta_y$ for which the laser is in normal incidence plotted against mirror position. The measured data is fitted with a linear function whose slope is the inverse of the mirror's radius of curvature. The RoC measured is of 7.95 meters.

allows for measurements with sub-ppm accuracy.

If none of the two options for mirror transmission measurements mentioned above are available, it is still possible to estimate it using the technique detailed by Isogai et al[17]. This technique considers a strongly over-coupled cavity but can easily be adapted to a cavity with symmetric transmission coefficients such as ours as explained in more detail in annex A.

### C. Mirror loss uniformity measurement

Before performing cavity loss measurements, the cavity input mirror is scanned over an area of 15 mm by 15 mm to ensure that during ring-down time measurements the intracavity beam is not incident on a mirror default at the input side of the cavity. The maximum scan range of the input mirror is limited to less than 15 mm due to the curvature of the mirror which requires it to be tilted as its position is scanned in order to preserve cavity alignment. This tilt induces a deviation of the reflected beam used for locking the laser frequency that requires manual compensation using a steering mirror placed in front of the PDH photodiode. For this reason, in this article only the end mirror position is scanned during cavity loss measurements.

Figure 6 shows the typical ring-down signal recorded at the output of the optical cavity

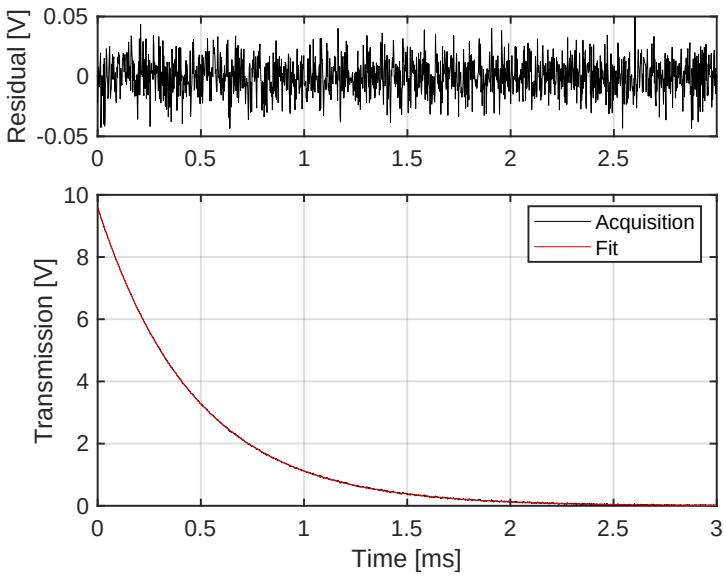


FIG. 6. Typical ring-down signal recorded at the output of the two-mirror cavity. The ring-down time of the cavity for this mirror position is of 466µs.

for an end-mirror position for which cavity ring-down time is of 466 µs. The first 10 µs immediately after the laser shutoff are removed from the analysed data to avoid potential response-time related effects from the photodiode due to discontinuities in the recorded signal. There is a very good correspondence between the recorded signal (black line) and exponential decay fit (red line) used to measure cavity ring-down time indicating the absence of parasitic phenomena that could affect ring-down time measurements.

Figures 7 and 8 depict total cavity losses and cavity finesse $F$ respectively as a function of end mirror position. Cavity Finesse, defined as the free spectral range of the resonator divided by the full width at half maximum of the cavity resonance, can be simplified for very low loss cavities as

$$F = \frac{2\pi}{L_{tot}} \tag{3}$$

Measurements were performed over a circular area of 22 mm in diameter with a step size of 0.73 mm which is smaller than beam spot radius of 1.05 mm measured at the output mirror positioning system using a knife edge method. A maximum finesse of 276 000 was measured corresponding to total cavity losses of 22.8 ppm including mirror transmission. The minimum finesse measured was of 30 000 corresponding to total cavity losses of 209 ppm. White regions in the losses/finesse maps correspond to regions on the mirror where no laser

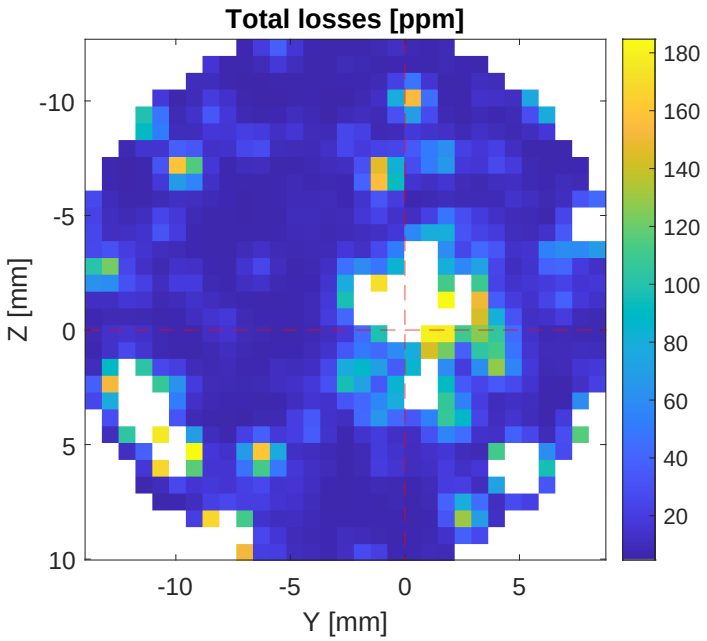


FIG. 7. Total cavity losses as a function of end mirror position.

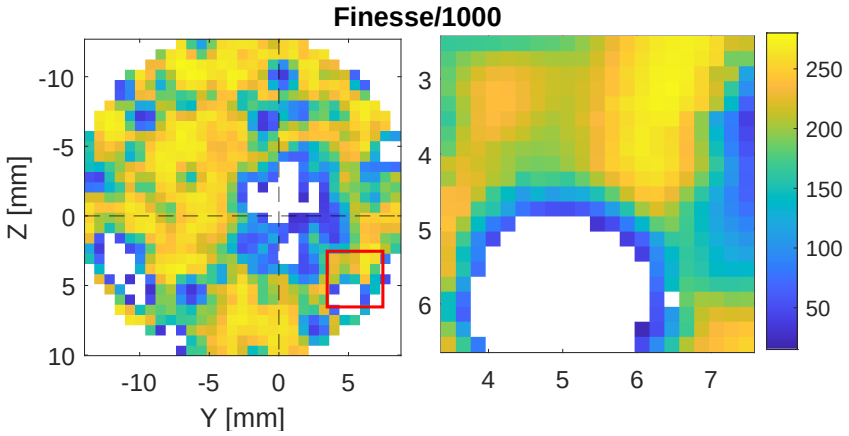


FIG. 8. Cavity finesse as a function of end mirror position. Left: 0.73 mm step-size used for mirror motion during measurements. Right: 0.2 mm step-size used for mirror motion around detected default

frequency locking could be performed due to very low cavity transmission. Losses in these regions are assumed to be higher than the maximum of 195 ppm as these positions are delimited by points corresponding to high cavity losses measured during the mirror scan.

While the spatial resolution of the measurement instrument is limited by the laser beam radius, the image resolution of the finesse maps can certainly be enhanced by using a smaller

step size. The map on the right side of figure 8 shows finesse measurements performed with a fine spatial step of 0.2 mm over a region of 4 mm by 4 mm delimited by the red square on the large-step-size finesse map. The defect detected is 2.2 mm large in the Y direction while its size in the z direction was not completely covered by the fine-step mirror scan. A good correspondence in color is observed between both maps showing a good measurement repeatability.

Excess losses are measured near the center of the mirror for both input and end mirrors. It is not inherent to the polishing process but rather linked to the cleaning procedure. Before coating, the substrate is cleaned on a spin coater with water and iso-propanol, unfortunately the curvature of the optics and the wettability of water on sapphire make the removal of residue in the center difficult.

Outside the center, the background of optical loss is compatible with superpolished optics with a roughness specified to be below 1 Å RMS.

### D. Cavity length scan

A unique new feature of the instrument is the possibility of longitudinal mirror displacement along the axis of the cavity. For specific cavity length, it is possible for high order optical modes to become resonant at the same time as the cavity fundamental mode[14]. The cavity is then said to be degenerated. Higher order optical modes are spatially larger in size and so present higher losses than the fundamental cavity mode. In this context, mode degeneracy can impact ring-down time measurements as the portion of light oscillating in the higher order mode will undergo stronger attenuation per roundtrip due to mirror clipping thus artificially increasing the value of the cavity optical loss.

Figure 9 shows total cavity losses measured via cavity ring-down time as a function of cavity length for scans of 10 mm and 5 mm using a step size of 0.025 mm showing no significant detrimental influence of higher order modes. It can be seen that the measurement is repeatable within 0.33 ppm. Over a scan of length 10 mm total cavity losses vary between 25 ppm and 27 ppm. A 1.8 ppm variation as measured in this cavity represents a variation of 7% about a point where losses were measured to be equal to 26.2 ppm. Numerical simulations using OSCAR have shown examples of more drastic losses occurring over smaller cavity length scans as can be seen in reference[18].

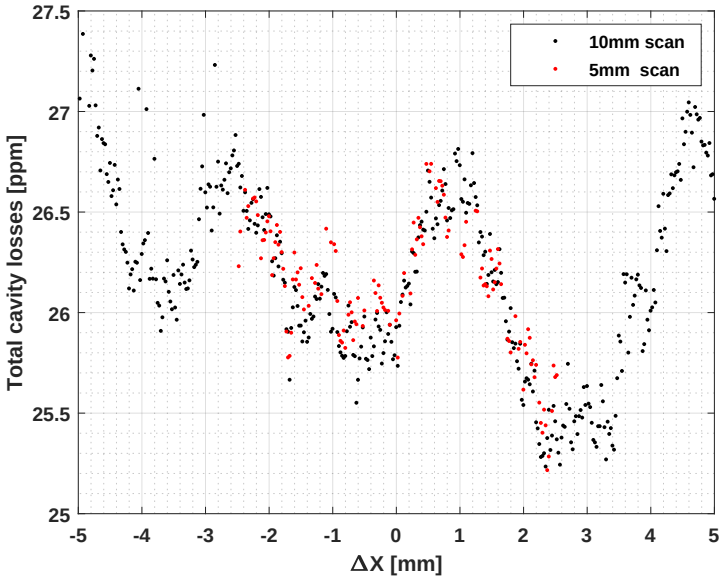


FIG. 9. Total cavity losses as a function of end mirror position along the cavity axis.

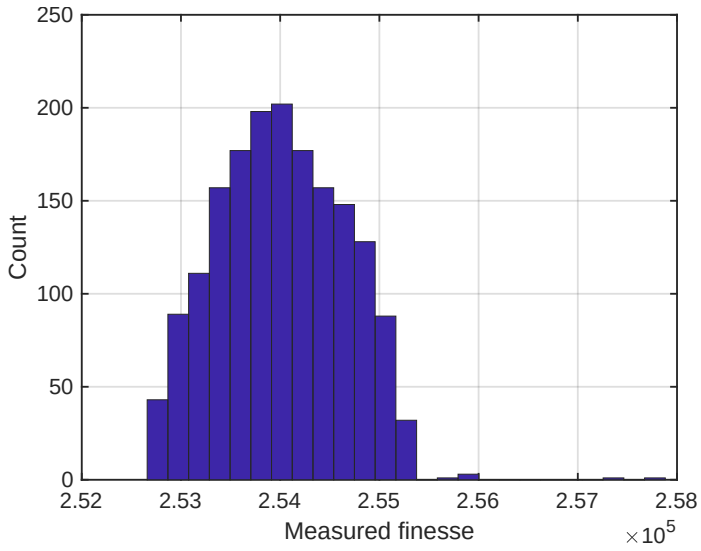


FIG. 10. Histogram of 1700 finesse measurements at a fixed mirror position. Mean finesse measured is 254000 with a standard deviation of 640

### E. Measurement repeatability

Measurement repeatability was tested by measuring ring-down time repeatedly at the same output mirror position over several hours. Figure 10 shows a histogram of 1700 finesse measurements.

The average finesse measured is of 25400 with a standard deviation of 640 or 2.5% which

translates to mean total losses of 24.7 ppm and a standard deviation of under 0.1 ppm over 1700 ring-down time measurements. This excellent repeatability of the ring-down time measurement can be owed to the method's insensibility of amplitude noise from the laser.

## V. CONCLUSION AND OUTLOOK

We developed an instrument that allows for the complete characterization of mirror coatings. Mirror losses can be measured under realisitc experimental conditions with this test bench. Transmission and radius of curvature of mirrors can be obtained using this bench for a full charaterization of mirrors which is of great interest for coating facilities. Mirror positioning with 6 degrees of freedom has allowed for changes of cavity length in order to test the presence of degenerated higher order optical modes that could potentially skew measured round trip losses in cavity characterization. Mirror transmission measurements were compared to measurements based on a CASI instrument and found to be compatible within 0.3 ppm. An alternative transmission measurement method was also presented for cavities with equal transmission mirrors. In the future, the instrument will be equipped with remote-controlled polarizers at the input and output of the cavity. This upgrade will allow us to take advantage of the remote controlled rotation stages upon which the mirrors are mounted and perform mirror coating birefringence measurements based on the polarimetry setups developed by the BMV[19] and PVLAS[20] teams. The final objective being the development of an instrument capable of mapping optical losses and birefrignence of very high reflectivity mirrors coated at LMA.

## 'ACKNOWLEDGEMENTS

The authors would like to thank Carlo Rizzo and Mathilde Fouché for their valuable contributions in the early development stages of the instrument.

This work was funded within the OSAG project thanks to the IDEXLYON from University of Lyon (Programme Investissements d'Avenir ANR-16-IDEX-0005).


FIG. 11. Schematic of a 2 mirror cavity. $a_0$ represents the incident optical field at the input side of the cavity, assumed to be perfectly coupled to the cavity fundamental mode. $b_0$ represents the reflected optical field at the input of the two-mirror cavity. The parameter $a_2$ represents the optical field transmitted through the cavity. Parameters $r, t, l$ represent the reflection, transmission and losses coefficients of the cavity mirrors.

## Appendix A: Mirror transmission and cavity coupling measurements

In this appendix we present a third technique to measure in-situ the transmission of the cavity mirrors. It is suitable for cavities with symmetric mirrors and adapted from the work of Isogai et al.[17]. The most interesting and practical aspect about this technique lays in its implementation since it can be achieved with the use of a single photodetector positioned in reflection of the cavity. In our experimental setup, the measurement is performed with the photodiode used to derive the PDH error signal which has also a DC output. Hence the technique proposed required no modification of the optical setup.

For the sake of clarity, the optical fields at the input and output of the cavity are labeled as depicted in figure 11. The part of the input optical field that can be coupled into the cavity is labeled $a_0$ corresponding to a CW laser signal of power $P_0 = |a_0|^2$. The optical field labeled $b_0$ represents the optical field reflected from the cavity. The transmitted optical field is labeled here $a_2$. Both input and end mirror are assumed to be identical and thus have the same reflectivity $r$, transmission $t$ and loss $l$ in amplitude. This is a reasonable assumption since both mirrors were polished in the same batch and coated in the same run.

Based on these assumptions and using the above notations, total cavity losses $L_{cav}$, transmission $T_{cav}$ and reflection $R_{cav}$ of the cavity as a function of the mirrors' properties and laser detuning $\delta$ are given by the system of equations:

$$
\begin{aligned}
T_{cav} &= \frac{|a_2|^2}{|a_0|^2} = \frac{|t^2 e^{-i\delta}|^2}{|1 - r^2 e^{-i\delta}|^2} \\
R_{cav} &= \frac{|b_0|^2}{|a_0|^2} = \frac{|r[1 - (t^2 + r^2)e^{-i\delta}]|^2}{|1 - r^2 e^{-i\delta}|^2} \\
L_{cav} &= 2(l^2 + t^2) = \frac{1}{\tau FSR} \\
1 &= r^2 + t^2 + l^2
\end{aligned}
\tag{A1}
$$

This is a system of 4 independent equations with 4 unknowns $r, t, l$ and $\delta$ which could be solved numerically. In the next paragraphs, we show how we can experimentally measure $T_{cav}, R_{cav}$ and $L_{cav}$ using the single PDH photodiode in reflection.

The first step in our analysis is to normalise the voltage from the PDH photodiode with respect to the input power laser beam. This is achieved by unlocking the cavity, in which case the reflectivity of the cavity is 100% and so all the input laser light is incident on the photodiode. The second step is to estimate the input power light that effectively couples to the cavity. In fact, some part of the input light remains out of resonance when the laser frequency is locked to the cavity due to two different mechanisms. First, the generation of a PDH error signal for laser frequency locking requires phase modulation of the input light which creates sidebands whose frequency-shift is by design out of resonance. In addition to this, due to small residual mode mismatching, a fraction of the input light does not couple to the cavity fundamental mode. Both of these quantities can be measured a priori with the use of a low finesse cavity ($F = 1000$) as described in appendix B.

The power carried by the sidebands represents 32% of the total reflected optical power while losses due to mode mismatch account for 8% of the total laser input power. These values represent an offset in the reflected power, as even for a symmetric loss-less on resonance cavity, 40% of the light will still be reflected by the cavity. After this subtraction, the estimated normalised reflected power $|b_0|^2/|a_0|^2$ of the cavity is measured to be 53.7%.

Since the cavity is symmetric, the transmitted power can also be derived from the reflected power. Once the laser is switched off, the field immediately leaking from the cavity's input mirror is the same in reflection and transmission. The normalised transmitted power when the cavity is locked $|a_2|^2/|a_0|^2$ is measured to be 23.7% by taking the last recorded point before laser shutoff as depicted in the right panel of figure 12. Fluctuations of the reflected laser light observed before the laser shutoff are due to instabilities of the laser frequency

that cannot be corrected by the PDH control loop. Finally, fitting the ringdown time in reflection gives us the total cavity round trip loss, including the transmission and the losses from the mirrors. So for the particular incident point with the data from figure 12, the previous system of equations satisfies:

$$\begin{aligned} T_{cav} &= 23.7\% \\ R_{cav} &= 53.7\% \\ L_{cav} &= 21.5ppm \\ 1 &= r^2 + t^2 + l^2 \end{aligned} \tag{A2}$$

The system of equations A1 can then be solved for $t^2$ and $\delta$ using a nonlinear solver from MATLAB which yields a result of $t^2 = 7.3\,\text{ppm}$ and a detuning $\delta$ =145 Hz which is close to a half cavity linewidth meaning that cavity transmission at this point is about 50% of transmission at resonance. A difference of about 11% (1 ppm) is found between this transmission measurement and CASI measurements. While CASI measurements are more reliable, in the absence of such a device, the technique presented in this section can serve as an alternative for transmission measurements of ultra-high reflectivity mirrors. The reason for the non-zero cavity detuning is not fully known, we believe that parasitic etalon effects cause residual amplitude modulation in the EOM used to generate the PDH error signal. This in turn may introduce a parasitic DC component in the PDH error signal causing a slight deviation of the central laser frequency with respect to the cavity resonance when the frequency control loop is on and the laser frequency is locked to the cavity resonance.

## Appendix B: Cavity length measurement and geometrical properties

An estimation of the cavity length can be obtained by scanning the laser frequency in presence of sidebands across a cavity FSR and recording the transmitted optical signal. The measurement is performed by applying a ramp voltage to the PZT in the laser head, assuming the latest to have a linear response.

The very high finesse cavity presented in the main text is not well suited for performing this measurement as the cavity response time is too long compared to the laser frequency drift. Lower reflectivity mirrors were used to create a low finesse cavity ($F = 1000$) that

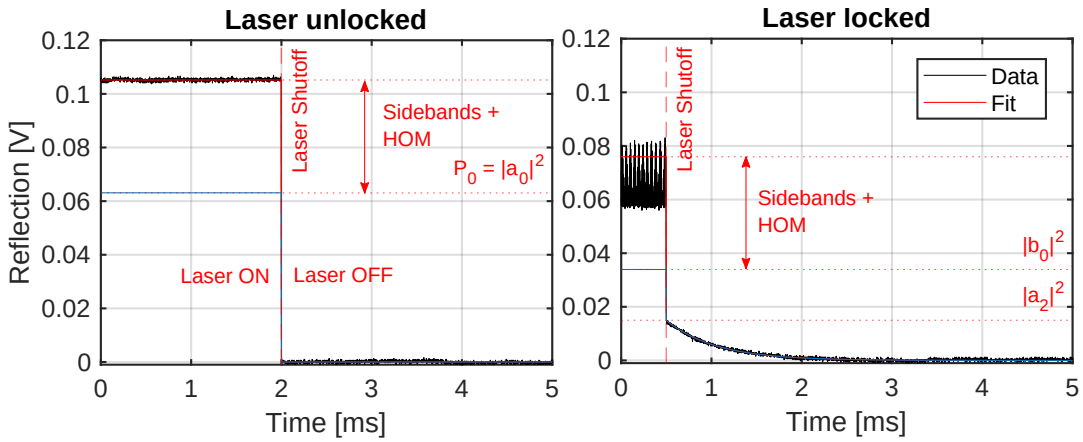


FIG. 12. PDH photoiode signal when the laser is on (right) and off (left) resonance. The recorded data is plotted in black lines and a least square fit is given in red. The blue lines represent the reflected optical power after subtraction of the sideband and HOM power that cannot be coupled into the cavity.

has a much broader linewidth. These lower reflectivity mirrors were polished to the same RoC specifications and by the same polisher as the mirrors presented in the main text and thus both the low and high finesse cavities possess the same geometrical properties. Once the cavity length is known, the low finesse cavity can also be used to measure mirror radius of curvature as well as mode mismatch.

Figure 13 shows the signal detected at the output of the cavity over a rising ramp of the voltage applied to the piezo crystal of the laser. The two highest peaks, indicated by the "Mode 00" markers, correspond to the resonance of the carrier fundamental mode. The smaller peaks that appear symmetrically next to the two highest peaks correspond to the modulation sidebands resonance fundamental mode. The height of the modulation sidebands can be measured here to estimate their optical power with respect to the carrier component of the laser.

Furthermore, since the phase modulation frequency $f_{mod}$ is very well defined, the distance between carrier and sidebands in this signal provides a frequency standard for measuring the cavity $FSR$ and thus length. The smaller peaks indicated by the markers "Mode 01" and "Mode 02" in figure 13 appear when the carrier component resonates with higher order modes 01 and 02 of the cavity. Odd higher order modes can be minimized by tilting the cavity mirrors until achieving close to perfect alignment. However, the presence of even

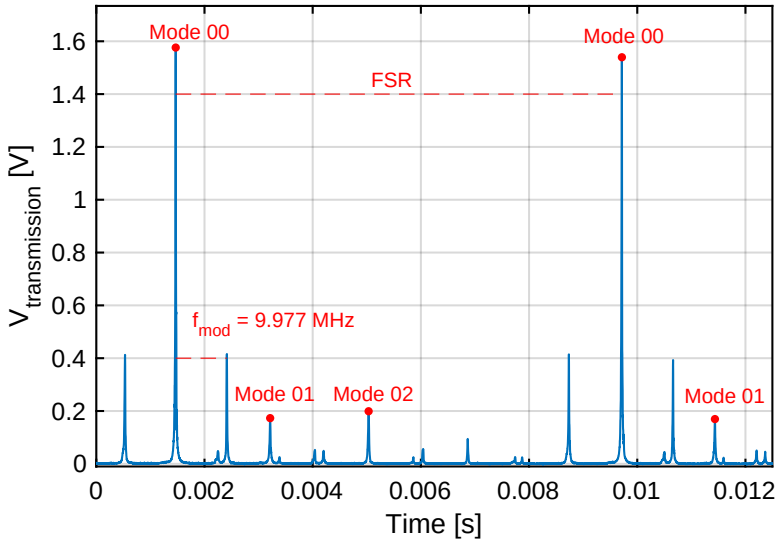


FIG. 13. Photodetected signal at the output of the low finesse cavity as the carrier frequency of a phase-modulated laser is scanned over a cavity $FSR$. The fundamental mode is surrounded by symmetrically spaced modulation sidebands created by the EOM. The first and second order modes of the cavity are indicated by red markers. The first order mode can be identified experimentally because it can be strongly attenuated with good cavity alignment. Mode 02 can be identified because it is separated from mode 00 by twice the spacing of mode 01. The modulation frequency $f_{mod}$ is known and provides a frequency standard for the measurement of the cavity FSR as well as first order mode spacing.

higher order modes depends on the cavity geometry as well as beam shape and cannot be completely eliminated by tilting the cavity mirrors. We use the method presented here to measure the amplitude of the second order mode of the cavity relative to the cavity fundamental mode which allows us to estimate the optical power that cannot be coupled into the cavity due to mode mismatch, a quantity that has to be known when using the method presented in Annex A to measure mirror transmission. Using a 160 Hz triangle-wave signal to scan the laser carrier frequency, a mean cavity length of 1.80 m was measured over 630 scans with a standard deviation of 6 mm. This measurement is consistent with manual measurements of cavity length using a measuring tape and telemeter. Because both mirrors were polished to the same specified radius of curvature of 8 m on the same batch, their radius of curvature can be obtained by measuring the frequency spacing between the cavity's fundamental mode and first order mode to obtain the cavity $g$ factor. A mean radius

of curvature of 7.84 m with a standard deviation 0.148 m was measured using this method, to be compared with the value measured in section IV A of 7.95 m.

## BIBLIOGRAPHY

## REFERENCES


[1]J. Liu, T. Liu, L. Chen, L. Zhang, G. Xu, D. Jiao, and S. Zhang, "A compact sub-hertz linewidth fabry perot cavity frequency stabilized laser for space application," Optics & Laser Technology **136**, 106777 (2021).

[2]F. Marino, F. S. Cataliotti, A. Farsi, M. S. de Cumis, and F. Marin, "Classical signature of ponderomotive squeezing in a suspended mirror resonator," Physical review letters **104**, 073601 (2010).

[3]F. a. Acernese, M. Agathos, K. Agatsuma, D. Aisa, N. Allemandou, A. Allocca, J. Amarni, P. Astone, G. Balestri, G. Ballardin, *et al.*, "Advanced virgo: a second-generation interferometric gravitational wave detector," Classical and Quantum Gravity **32**, 024001 (2014).

[4]J. Degallaix, C. Michel, B. Sassolas, A. Allocca, G. Cagnoli, L. Balzarini, V. Dolique, R. Flaminio, D. Forest, M. Granata, *et al.*, "Large and extremely low loss: the unique challenges of gravitational wave mirrors," JOSA A **36**, C85–C94 (2019).

[5]C. Karras, "Cavity ring-down technique for optical coating characterization," in *Optical Characterization of Thin Solid Films*, edited by O. Stenzel and M. Ohlídal (Springer International Publishing, 2018) pp. 433–456.

[6]Y. Han, B. Li, G. Lifeng, and S. Xiong, "Reflectivity mapping of large-aperture mirrors with cavity ringdown technique," Applied Optics **56**, C35–C40 (2017).

[7]H. Cui, B. Li, S. Xiao, Y. Han, J. Wang, C. Gao, and Y. Wang, "Simultaneous mapping of reflectance, transmittance and optical loss of highly reflective and anti-reflective coatings with two-channel cavity ring-down technique," Optics Express **25**, 5807–5820 (2017).

[8]G.-W. Truong, G. Winkler, T. Zederbauer, D. Bachmann, P. Heu, D. Follman, M. White, O. Heckl, and G. Cole, "Near-infrared scanning cavity ringdown for optical loss characterization of supermirrors," Optics Express **27**, 19141–19149 (2019).

[9]R. Drever, J. L. Hall, F. Kowalski, J. Hough, G. Ford, A. Munley, and H. Ward, "Laser phase and frequency stabilization using an optical resonator," Applied Physics B **31**, 97–

105 (1983).

[10]E. D. Black, "An introduction to pound–drever–hall laser frequency stabilization," American journal of physics **69**, 79–87 (2001).

[11]E. A. Donley, T. P. Heavner, F. Levi, M. Tataw, and S. R. Jefferts, "Double-pass acousto-optic modulator system," Review of Scientific Instruments **76**, 063112 (2005).

[12]D. McCarron, "A guide to acousto-optic modulators," : http://massey. dur. ac. uk/resources/slcornish/AOMGuide. pdf (2007).

[13]"Sisyph signals & systems for physics," `http://www.sisyph.com/` (2022).

[14]L. Amoudry, H. Wang, K. Cassou, R. Chiche, K. Dupraz, A. Martens, D. Nutarelli, V. Soskov, and F. Zomer, "Modal instability suppression in a high-average-power and high-finesse fabry–perot cavity," Applied Optics **59**, 116–121 (2020).

[15]"Coastline optics," `http://www.coastlineoptics.com/` (2022).

[16]L. Pinard, C. Michel, B. Sassolas, J. Teillon, G. Cagnoli, M. Sigwarth, T. Kentischer, W. Schmidt, and B. Reichman, "High uniformity ibs coatings for the world's largest fabry-perot etalon of the vtf instrument," in *Advances in Optical and Mechanical Technologies for Telescopes and Instrumentation III*, Vol. 10706 (SPIE, 2018) pp. 526–533.

[17]T. Isogai, J. Miller, P. Kwee, L. Barsotti, and M. Evans, "Loss in long-storage-time optical cavities," Optics express **21**, 30114–30125 (2013).

[18]J. Degallaix, "A tale of two cavities," (2021).

[19]M. T. Hartman, R. Battesti, and C. Rizzo, "Characterization of the vacuum birefringence polarimeter at bmv: dynamical cavity mirror birefringence," IEEE Transactions on Instrumentation and Measurement **68**, 2268–2273 (2019).

[20]A. Ejlli, F. Della Valle, U. Gastaldi, G. Messineo, R. Pengo, G. Ruoso, and G. Zavattini, "The pvlas experiment: A 25 year effort to measure vacuum magnetic birefringence," Physics Reports **871**, 1–74 (2020).